

SINGLE TREE DETECTION IN FOREST AREAS WITH HIGH-DENSITY LIDAR DATA

J. Reitberger^{a,*}, M. Heurich^b, P. Krzystek^a, U. Stilla^c

^a Dept. of Geoinformatics, Munich University of Applied Sciences, 80333 Munich, Germany
(reitberger, krzystek)@fhm.edu

^b Dept. of Research, Bavarian Forest National Park, 94481 Grafenau, Germany
Marco.Heurich@npv-bw.bayern.de

^c Photogrammetry and Remote Sensing, Technische Universitaet Muenchen, 80290 Munich, Germany
stilla@tum.de

Commission III, WG III /3

KEY WORDS: LIDAR, analysis, segmentation, forestry, vegetation

ABSTRACT:

The study presents a novel method for delineation of tree crowns and detection of stem positions of single trees from dense airborne LIDAR data. The core module of the method is a surface reconstruction that robustly interpolates the canopy height model (CHM) from the LIDAR data. Tree segments are found by applying the watershed algorithm to the CHM. Possible stem positions of the tallest trees in the segments are subsequently derived from the local maxima of the CHM. Additional stem positions in the segments are found in a 3-step algorithm. First, all the points between the ground and the crown base height are separated. Second, possible stem points are found by hierarchical clustering these points using their horizontal distances. Third, the stem position is estimated with a robust RANSAC-based adjustment of the stem points. We applied the method to small-footprint full waveform data that have been acquired in the Bavarian Forest National Park with a point density of approximately 25 points per m². The results indicate that the detection rate for coniferous trees is 61 % and for deciduous trees 44 %, respectively. 7 % of the detected trees are false positives. The mean positioning error is 0.92 cm, whereas the additional stem detection improves the position on average by 22 cm.

1. INTRODUCTION

Laser scanning has become the leading edge technology for the acquisition of topographic data and the mapping of the Earth's surface and offers several advantages for forest applications. The laser beam may penetrate the forest structure, and the technique provides 3D information at a high point density and intensity values at a specific wavelength. Since over a decade, conventional LIDAR - recording the first and last pulse - has been widely used to successfully retrieve forest parameters like tree height, crown diameter, number of stems, stem diameter and basal area (Hyyppä et al., 2004). Recently, tree species classification could be tackled with first/last-pulse scanning systems providing high point density (Holmgren et al., 2004; Heurich, 2006; Brandtberg, 2007). Moreover, the novel airborne full waveform technology promising new possibilities has been lately applied to tree species classification (Reitberger et al., 2006).

Approaches to tree species classification are usually based on a single tree segmentation that delineates the tree crown from the outer geometry of the forest surface. The methods have in common to reconstruct – at least locally – the canopy height model (CHM) to find the local maximum in the CHM as the best guess for the stem position and to delineate a segment polygon as the tree crown. For instance, Hyyppä et al. (2001) interpolate a local CHM from the highest laser reflections, Persson et al. (2002) apply the active contour algorithm, and Solberg et al. (2006) interpolate the CHM with a special gridding method and subsequently smooth the CHM with an appropriate Gaussian filter. Stem positions are derived from the interpolated CHM at the highest positions (Solberg et al., 2006) or from a special local tree shape reconstruction (Brandtberg, 2007). Tree crowns are typically derived with the watershed

algorithm (Pyysalo et al., 2002) or by a slope-based segmentation (Persson et al., 2002; Hyyppä et al., 2001). Recently, Solberg et al. (2006) proposed a region growing method that starts from local surface maximums and finds crown polygons optimised in shape.

The drawback of these methods is that they are solely oriented on the CHM. The CHM is reconstructed from the raw data in an interpolation process that smoothes the data to some extent. The degree of smoothing affects directly the success rate in terms of false positives and negatives. Moreover, in some cases neighbouring trees do not appear as two clear local maximums. Thus, approaches that solely use the CHM will be restricted in the success rate anyway, especially in heterogeneous forest types where group of trees grow close together. So far, little attention has been paid to reconstruct trees using information like laser hits on the stem, mainly because of the low spatial point density. Detected tree stems could be used to improve the CHM-based segmentation of the single trees in terms of the detection rate of trees and the position of the trees. Moreover, new full waveform systems have the potential to detect significantly more reflections in the tree crown and hence highly resolve the internal tree structure.

The objective of this paper is (i) to present a novel method that segments single trees with a robust surface reconstruction method in combination with the watershed algorithm using full waveform LIDAR data, (ii) to introduce a novel approach to stem detection that clusters hierarchically potential stem reflections and reconstructs the stem with a RANSAC-based adjustment, and (iii) to show how the detection rate and position of single trees is improved.

The paper is divided into five sections. Section 2 focuses on the segmentation of the single trees and the reconstruction of the

* Corresponding author.

tree stems. Section 3 shows the results which have been obtained from full waveform data acquired in May 2006 by the Riegl LMS-Q560 system in the Bavarian Forest National Park. Finally, the results are discussed with conclusions in section 4 and 5.

2. METHODOLOGY

2.1 Decomposition of full waveform data

Let us assume that full waveform LIDAR data have been captured in a region of interest (ROI). The waveforms are decomposed by fitting a series of Gaussian pulses to the waveforms (Figure 1). Thus, for each reflection i the vector $\mathbf{X}_i^T = (x_i, y_i, z_i, W_i, I_i)$ ($i=1, \dots, N_{ROI}$) is provided with (x_i, y_i, z_i) as the coordinates, W_i as the pulse width and I_i as the intensity of the reflection (Reitberger et al., 2006; Jutzi and Stilla, 2005). Note that basically each reflection can be detected by the waveform decomposition. This is remarkable since conventional LIDAR systems – recording at most five reflections – have a dead zone of about 3 m which make these systems effectively blind after a single reflection.

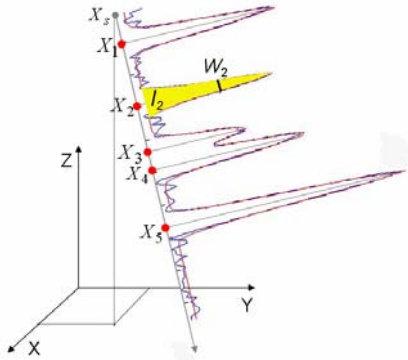


Figure 1. 3D points and attributes derived from a waveform

2.2 Segmentation

The segmentation of the tree crowns is achieved by deriving the CHM from 3D points which are best representing the outer tree crown geometry. The ROI is subdivided into a grid having a cell spacing of cp and N_R cells (Figure 2). Within each cell of size cp^2 , the highest 3D point is extracted and corrected with respect to the ground level z_j^{ground} , i.e.

$z_j^{CHM} = z_j - z_j^{ground}$ ($j=1, \dots, N_R$). The ground level z_j^{ground} is estimated from a given digital terrain model (DTM) by bilinear interpolation. In the next step, all the highest 3D points $\mathbf{X}_j^T = (x_j, y_j, z_j^{CHM})$ ($j=1, \dots, N_R$) of all N_R cells are robustly interpolated in a grid that has N_X and N_Y grid lines and a grid width gw . The special adjustment approach (Krzystek et al., 1992) interpolates the $N_{CHM} = N_X * N_Y$ grid points

$\mathbf{X}_{Int_j}^{CHM T} = (x_{Int_j}^{CHM}, y_{Int_j}^{CHM}, z_{Int_j}^{CHM})$ ($j=1, \dots, N_{CHM}$) and filters the 3D points \mathbf{X}_j in a 2-phase iterative Gauß-Markoff process. Thanks to constraints on the curvature and torsion of the surface, the interpolation smoothes and regularises the surface in case of an ill-posed local situation. Moreover, single outlying 3D points, which do not represent the CHM surface, are down-weighted by weighting functions in dependence on the distance of the 3D points to the surface. This iterative adjustment scheme works like an edge preserving filter that discards outliers, closes gaps in the surface if no 3D points could be

found in the cells, and preserves surface discontinuities. The result is a smoothed CHM having N_{CHM} equally spaced posts. Finally, the tree segments are found by applying the watershed algorithm (Vincent and Soille, 1991) to the CHM. The local maximums of the segments define the N_{seg} tree positions $(X_{stem_i}^{CHM}, Y_{stem_i}^{CHM})$ ($i=1, \dots, N_{seg}$).

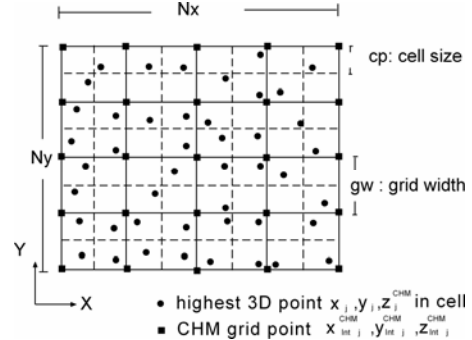


Figure 2. Finite element interpolation for a patch of 16 grid meshes

2.3 Stem detection

Tree stems in the individual tree segments are detected in a 3-step procedure.

Step 1: The N_S points X_j^{Seg} ($j=1, \dots, N_S$) within a tree segment are cleared from ground points by discarding all points within a given height bound $Z_{threshold} = 1$ m to the DTM.

Step 2: The goal of the second step is to derive the crown base height h_{base} of the tree in order to subdivide the tree into the stem area and the remaining crown area. This coarse tree subdivision is achieved by (i) splitting the tree into l layers with height of 0.5 m (Figure 3a), (ii) calculating the number of points n_i per layer, (iii) forming the vector $N_p = \{n_i / N_S\}$ ($i=1, \dots, l$), (iv) smoothing N_p with a 3x1 Gaussian filter and, finally, (v) defining h_{base} as the height that corresponds to 0.15 % of the total number of points per segment (Figure 3b). All the N_{stem} points below h_{base} are potential stem points. Note that the remaining points can result from one or even several stems or from the understorey. The following hierarchical clustering scheme is applied to these points after calculating the Euclidian

distance matrix $D_{stem} = \{d_{ij} = \sqrt{(x_i - x_j)^2 + (y_i - y_j)^2}\}$; $i=1, \dots, N_{stem}$; $j=1, \dots, N_{stem}$; $i \neq j$ (Heijden et al., 2004).

1. Assign each point to its own cluster, resulting in N_{stem} clusters.
2. Find the closest pair of clusters and merge them in to one cluster. The number of clusters reduces by one.
3. Compute the distance d between the new clusters and each of the old clusters.
4. Repeat steps 2 and 3 until all items are clustered into a single cluster of size N_{stem} or a predefined number of clusters is achieved.

In this clustering process the distance between two clusters C_i and C_j is defined as the shortest distance from any point in one cluster to any point in the other cluster. The clustering yields a dendrogram which shows at which distance the clusters are grouped together. By defining a minimum distance $d_{min} = 1.2$ m

between the cluster centres the most suitable number of clusters $N_{cluster}$ is selected.

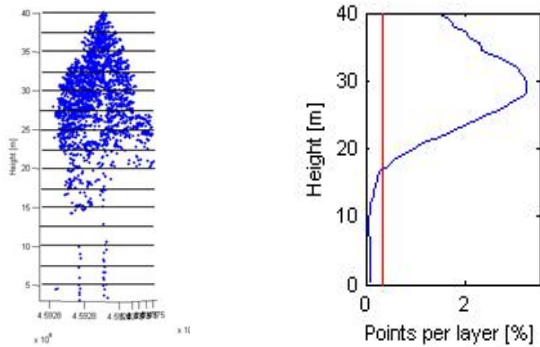


Figure 3a. Tree layers

Figure 3b. Base height of a tree

Step 3: The final finding of the stems is achieved by applying a RANSAC-based 3D line adjustment to all the $N_{cluster}$ clusters and labelling all 3D lines with an incident angle smaller than $\alpha = 7^\circ$ and a minimum number of 3 points as stems g_{stem} . This robust procedure eliminates clusters that result from the understory and do not show a vertical main direction. Also, it cleans the cluster point cloud from erroneous points. The stem positions $(x_{stem}^{det}, y_{stem}^{det})$ are calculated as the intersection of the stem g_{stem} with the DTM $(x_{stem}^{det}, y_{stem}^{det}) = \{DTM \cap g_{stem}\}$. Finally, the height of the tree top h_{tree} is derived from the highest laser point that lies within the cylinder V_{stem} . The cylinder V_{stem} is defined by the 3D line g_{stem} as the centre line of the cylinder and the radius $R = 1$ m. Note that several stems can be found within a tree segment. However, the tree height is dependent on the highest raw data within the stem cylinder V_{stem} .

3. EXPERIMENTS

3.1 Material

Experiments were conducted in the Bavarian Forest National Park which is located in south-eastern Germany along the border to the Czech Republic (49° 3' 19" N, 13° 12' 9" E). There are four major test sites of size between 591 ha and 954 ha containing alpine spruce forests, mixed mountain forests and spruce forests as the three major forest types. 11 sample plots with an area size between 1000 m² and 3600 m² were selected in the mixed mountain forests dominated by Norway spruce (*Picea abies*) and European beech (*Fagus sylvatica*). Some fir trees (*Abies alba*), Sycamore maples (*Acer pseudoplatanus*) and Norway maples (*Acer platanoides*) also occur in the sample plots. The height above sea level varies between 610 m and 770 m. Reference data for all trees with diameter at breast height (DBH) larger than 10 cm have been collected in May 2006 for 438 Norway spruces, 477 European beeches, 74 fir trees, 20 Sycamore maples and three Norway maples. Several tree parameters like the DBH, total tree height, stem position and tree species were measured and determined with the help of GPS, tacheometry and the 'Vertex' III system. Moreover, a DTM with a grid size of 1 m and an absolute accuracy of 25 cm was available for all the test sites. It was generated from LIDAR data which had been acquired in 2003 (Heurich, 2006). For two of the four test sites, which contain the 11 sample plots, full waveform data have been collected by Milan Flug GmbH with the Riegl LMS-Q560 scanner. The Riegl scanner was flown in May 2006 after snowmelt but prior to foliation. The vertical sampling distance was 15 cm because of the scanner's

sampling rate of 1 GHz. The pulse width at half maximum reached 4 ns which is equivalent to 60 cm. The size of the footprint of 20 cm was caused by the beam divergence of 0.5 mrad and the flying altitude of 400 m. Finally, the average point density was 25 points/m². Thorough calibration of the bore sight alignment and strip adjustment was carried out prior to the data evaluation. Controlled tests showed that the strips had been adjusted with a standard deviation of 15 cm in planimetry and 10 cm in height. The procedures for segmentation and subsequent stem detection were applied to all the plots in a batch procedure without any manual interaction.

3.2 Segmentation

Figures 4 and 5 show a typical sample area containing several coniferous trees. The tree tops derived from the local maximums of the CHM correspond in some cases with the reference trees reasonably. However, some tree tops are deviating considerably from the true position. Moreover, some segments contain more than one reference tree although only one tree top has been derived from the CHM. The main reasons are that (i) a group of trees form locally a well-defined maximum and (ii) the surface reconstruction smoothes the surface too much so that neighbouring trees cannot be isolated. In both cases the single trees are not detected and hence the segment represents a group of trees rather than a single tree.

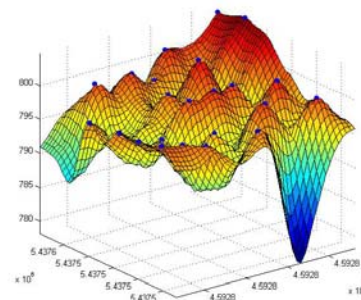


Figure 4. Reconstructed CHM with local maximums as tree tops

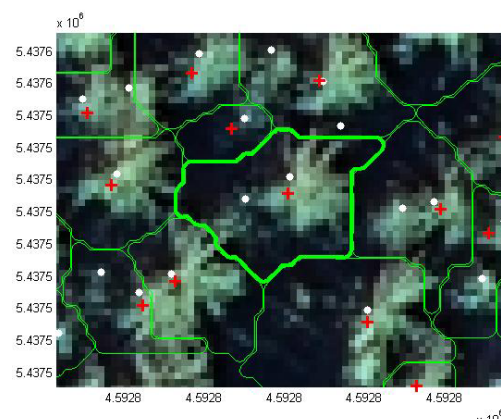


Figure 5. Orthophoto with sample segment containing two reference coniferous trees (=white dots) and one local maximum (=red cross)

3.3 Stem detection

The stem detection takes advantage of additional high-density point information the waveform decomposition provides underneath the CHM. In case that only sparse understory is below the base height stem points are successfully detected by

the hierarchical clustering and the RANSAC-based stem reconstruction. Figures 6a and 6b show the stem points for the sample segment in figure 5 found by the clustering scheme given in section 2.3. The two stems are clearly isolated by applying the angle constraint of 7^0 to the stems approximated with RANSAC. Moreover, the single stem position derived from the CHM maximum is significantly improved by the new stem position (Figure 7). Also, some neighbouring segments show similar results. For example, in the segment directly above the central segment even 3 stems could be detected whose positions correspond fairly well with the reference trees. Thus, the stem detection provides additional single trees that cannot be found solely using the CHM information and improves the position of trees derived from the CHM maximum.

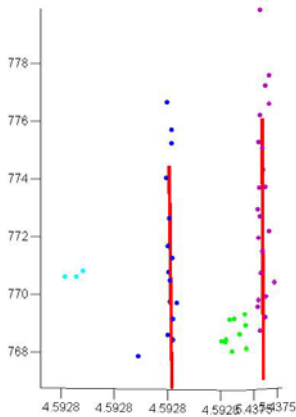


Figure 6a. Stem point clusters and stems reconstructed with RANSAC

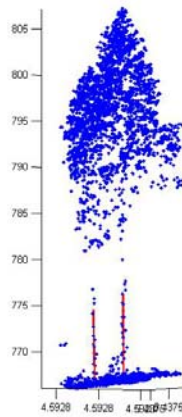


Figure 6b. The neighbouring trees and the reconstructed stems

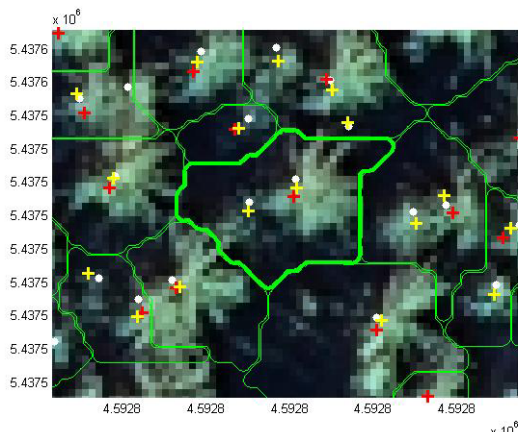


Figure 7. Sample segment with two reference coniferous trees (=white dots), two detected stems (=yellow crosses) and the local CHM maximum (=red cross)

3.4 Evaluation

The tree positions $(x_{stem}^{CHM}, y_{stem}^{CHM})$ from the segmentation and the tree positions $(x_{stem}^{det}, y_{stem}^{det})$ from the stem detection are compared with reference trees if (i) the distances to the reference trees is smaller than 60 % of the mean tree distance of the plot and (ii) the height difference between h_{tree} and the height of the reference tree is smaller than 15 % of the top height h_{top} of the plot, where h_{top} is defined as the average

height of the 100 highest trees per ha (Heurich, 2006). If a reference tree is assigned to more than one tree position, the tree position with the minimum distance to the reference tree is selected. Reference trees that are linked to one tree position are so-called “detected trees” and reference trees without any link to a tree position are treated as “non-detected” trees. Finally, a tree position without a link to a reference tree results as a “false detected” tree.

3.5 Results

Table 1 contains the percentage of “detected” trees for each plot. The trees are subdivided into 3 layers with respect to h_{top} . The lower layer contains all trees below 50 % of h_{top} , the intermediate layer refers to all trees between 50 % and 80 % of h_{top} , and, finally, the upper layer contains the rest of the trees.

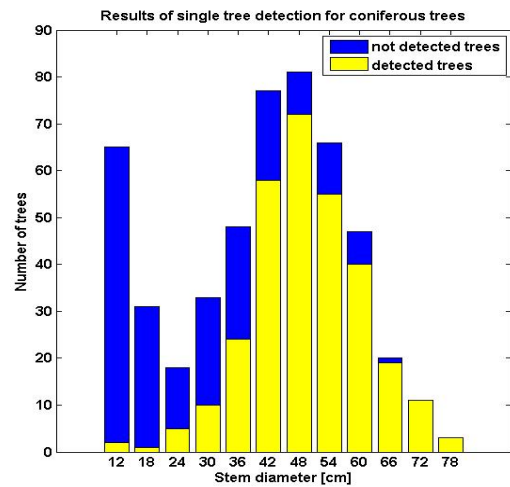


Figure 8. Number of detected coniferous trees in dependence on the DBH

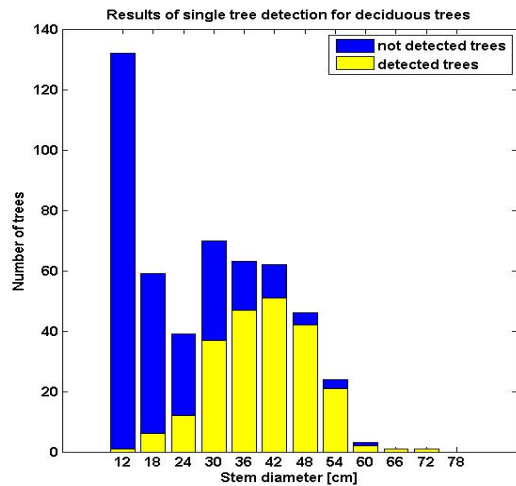


Figure 9. Number of detected deciduous trees in dependence on the DBH

First, we evaluate the detection rate of trees that are derived from the CHM without stem detection and hence refer to a local maximum in the CHM. Table 1 shows in general that most of the detected trees are in the upper layer. The detection rate varies between 56 % and 94 % while the overall detection rate for all plots amounts to 74 %. In comparison, in the intermediate layer and lower layer the detection rate is considerably smaller. Especially, in the lower layer only a few trees can be found since most of these trees are covered by

taller trees. The mean number of false detected trees amounts to 5 % and indicates a remarkable reliability. When applying the stem detection we get an overall improvement of the detection rate in the intermediate layer of 8 % and in the upper layer of 4 %. However, no improvement is achieved in the lower layer since (i) laser hits at the stem of small trees happen rarely, (ii) the base height h_{base} is inaccurate for trees beneath taller trees, and (iii) some trees have no clear base height since their green branches start close to the ground.

Moreover, the improvement of the detection rate is different in the individual plots. For instance, in the plots 55, 56, 58 and 81 (multi-layered stands), which contain more trees in the lower layer, no additional stems could be detected, whereas the plots 57 and 74 are significantly improved with more than 15 %. In general, the number of false detected trees gets slightly larger, most notably in the plot 93. Finally, the figures 8 and 9 show clearly that the detection rate of trees with a larger stem diameter at breast height (DBH) is considerably high for coniferous and deciduous trees. On average, the detection rate for coniferous trees is 61 % and for deciduous trees 44 %, respectively. Finally, table 2 shows the absolute positional improvement of the trees derived from the stem positions $(x_{stem}^{det}, y_{stem}^{det})$ and the position of the reference trees. As expected, the mean positioning error of deciduous trees gets better by 26 % which corresponds to 43 cm. The overall improvement of the tree position amounts to 24 cm which is equivalent to 21 %.

	Without "stem detection"	With "stem detection"
Mean positioning error coniferous	0.80 m	0.70 m
Mean positioning error deciduous	1.65 m	1.22 m
Total mean positioning error	1.16 m	0.92 m

Table 2. Accuracy of the tree position without and with stem detection

4. DISCUSSION

Conceptually, the presented approach to single tree detection from airborne LIDAR data goes one step further than existing methods by using the CHM and additional information inside the tree. It leads to an improvement of the detection rate of single trees in the intermediate and upper forest layer by detecting tree stems. This refinement of the detection rate could be expected since (i) in many cases neighbouring trees do not appear as two clear maximums in the raw data and (ii) the smoothing of the CHM blurs the maximums. Apparently, as already pointed out by some other authors (e.g. Solberg et al., 2006), the smoothing of the reconstructed CHM influences the quality of the single tree detection considerably. In general, a strong smoothing deteriorates the detection rate but decreases the number of false detected trees. However, a slight smoothing is necessary to avoid the finding of several wrong local maximums in one tree. Note that the surface reconstruction method in our approach works like an edge preserving filter which automatically adapts to local surface structures. However, a weak smoothing factor of 0.3 is still needed since otherwise the surface gets too noisy. The second advantage of the presented method is that the position of detected trees is significantly improved. This is also not very surprising since the

intersection of the detected tree stem with the DTM must be more precise than the tree position derived from the CHM maximum. Thirdly, the stem detection checks the hypothesis of stem positions which have been derived from the CHM. The restrictions of the approach are that only trees in the upper and intermediate forest layer can be additionally detected. It fails in the lower layer where stem hits are rare and stems points can not be clearly clustered. Also, the tree height still depends on the highest point found in the raw data contained in the stem cylinder V_{stem} . Thus, in all cases where the tree belonging to the detected stem is covered by a taller tree the derived tree height h_{tree} can be erroneous. Moreover, so far we have not implemented to go back to the raw data and to find a new segmentation of the tree crowns using the stem information.

Heurich (2006) reported recently on segmentation results using conventional first/last pulse data captured – like our data – in the Bavarian Forest National Park. He applied the segmentation approach developed by Persson et al. (2002). In detail, the detection rates for coniferous trees were 51%, for deciduous trees 40 %, and on average 45 %. These results are slightly worse than our results, but cannot be directly compared, because the test plots of that study were not exactly the same. However, the comparison is important since it refers to the same forest type. The study of Persson et al. (2002) reports on a detection rate of 71 % of all trees with a DBH larger than 5 cm for a Scandinavian forest dominated by spruce and pine. The positional accuracy of the stem positions was 51 cm. Recently, Solberg et al. (2006) presented a study for a structurally heterogeneous spruce forest with an overall detection rate of 66 % and commission rate (=false detections) of 26 % if the CHM is smoothed 3 times with a Gaussian filter of size 30 cm.

5. CONCLUSIONS

The study presents a novel single tree detection based on a combined surface reconstruction and stem detection. The results attained in heterogeneous forest types show clearly that the detection rate and position of single trees can be improved in the upper and intermediate layer. Future research should be focussed on (i) the improvement of the segmentation of the tree crowns using the stem information (ii) the analysis of the point's intensity and pulse width the waveform decomposition provides. More important, a rigorous 3D segmentation of the trees based on the points and the intensity and pulse width should be tackled to fully reconstruct the trees even in the lower layer.

6. LITERATURE

Brandtberg, T., 2007, Classifying individual tree species under leaf-off and leaf-on conditions using airborne lidar. *ISPRS Journal of Photogrammetry and Remote Sensing*, 61, pp. 325 – 340.

Heijden, F. van der, Duin, R.P.W., Ridder, D. de, Tax, D.M.J., 2004. *Classification, parameter estimation and state estimation – An engineering approach using MATLAB*. John Wiley & Sons Ltd, The Attriium, southern Gate, Chichester, West Sussex PO19 8SQ, England.

Heurich, M., 2006, Evaluierung und Entwicklung von Methoden zur automatisierten Erfassung von Waldstrukturen aus Daten flugzeuggetragener Fernerkundungssensoren. *Schriftenreihe des Wissenschaftszentrums Weihenstephan für*

Ernährung, Landnutzung und Umwelt der Technischen Universität München und der Bayerischen Landesanstalt für Wald und Forstwirtschaft, Forstlicher Forschungsbericht München, Nr. 202, ISBN 3-933506-33-6. <http://meadiatum2/ub.tum.de/> (Accessed February 18, 2007).

Holmgren, J., Persson, Å., 2004, Identifying species of individual trees using airborne laser scanner. *Remote Sensing of Environment* 90 (2004) 415-423.

Hyypä, J., Hyypä, H., Litkey, P., Yu, X., Haggren, H., Rönholm, P., Pyysalo, U., Pikänen, J., Maltamo, M., 2004, Algorithms and methods of airborne laser scanning for forest measurements. *Proceedings of the ISPRS working group VIII/2 Laser-Scanners for Forest and Landscape Assessment*, Volume XXXVI, PART 8/W2, 3 – 6th October, Freiburg, pp. 82 – 89.

Hyypä, J., Kelle, O., Lehtikoinen, M., Inkinen, M., 2001. A segmentation-based method to retrieve stem volume estimates from 3-D tree height models produced by laser scanners. *IEEE Transactions on Geoscience and Remote Sensing*, 39:969-975.

Jutzi B., Stilla U. 2005. Waveform processing of laser pulses for reconstruction of surfaces in urban areas. In: Moeller M, Wentz E (eds) 3th International Symposium: Remote sensing and data fusion on urban areas, URBAN 2005. International Archives of Photogrammetry and Remote Sensing. Vol 36, Part 8 W27.

Krzystek, P., Wild, D., 1992, Experimental accuracy analysis of automatically measured digital terrain models. *Robust*

Computer Vision: Quality of vision algorithms. Förstner, Ruhwedel (ed.). Wichman Verlag, Karlsruhe, pp. 372 -390.

Persson, A., Holmgren, J. and Söderman, U., 2002. Detecting and measuring individual trees using an airborne laserscanner. *Photogrammetric Engineering & Remote Sensing* 68(9), pp. 925–932.

Pyysalo, U., Hyypä, H., 2002. Reconstructing Tree Crowns from Laser Scanner Data for Feature Extraction. In *ISPRS Commission III, Symposium 2002 September 9 - 13, 2002, Graz, Austria*, pages B-218 ff (4 pages).

Reitberger, J., Krzystek, P., Stilla, U. 2006. Analysis of Full Waveform Lidar Data for Tree Species Classification. *Symposium ISPRS Commission III "Photogrammetric Computer Vision" PCV06*, 20 – 22th September, Bonn, Germany.

Solberg, S., Naesset, E., Bollandsas, O. M., 2006. Single Tree Segmentation Using Airborne Laser Scanner Data in a Structurally Heterogeneous Spruce Forest. *Photogrammetric Engineering & Remote Sensing*, Vol. 72, No. 12, December 2006, pp. 1369-1378.

Vincent, L., Soille, P., 1991, Watersheds in Digital Spaces: An Efficient Algorithm Based on Immersion Simulations. *IEEE Transactions of Pattern Analysis and Machine Intelligence*, Vol. 13, No. 6, June 1991, pp. 583-598.

Plot	55	56	57	58	74	81	91	92	93	94	95	All plots	
Average age [years]	240	170	100	85	85	70	110	110	110	110	110		
Size [ha]	0.14	0.23	0.10	0.10	0.30	0.30	0.36	0.25	0.28	0.29	0.25	2.60	
Number of trees per ha	830	340	450	440	700	610	260	170	240	250	240	390	
Number of trees in lower layer	76	31	0	10	11	29	31	13	7	15	6	229	
Number of trees in intermediate layer	22	19	4	4	33	59	11	3	2	4	0	161	
Number of trees in upper layer	18	27	41	30	165	96	53	27	58	54	53	622	
Percentage of deciduous [%]	5	10	0	14	29	100	76	100	64	97	10	49	
Without "stem detection"	Detected trees lower layer [%]	1	7	0	0	0	7	8	0	0	0	3	
	Detected trees intermediate layer [%]	32	42	25	25	6	9	0	50	0	0	13	
	Detected trees upper layer [%]	56	74	81	73	69	85	85	72	94	89	74	
	Total number of detected trees [%]	16	39	76	52	55	30	51	56	64	70	80	49
	False detected trees [%]	1	1	0	0	1	8	8	19	9	7	3	5
With "stem detection"	Detected trees lower layer [%]	1	7	0	0	0	7	8	0	0	0	3	
	Detected trees intermediate layer [%]	32	42	75	25	30	9	33	100	0	0	21	
	Detected trees upper layer [%]	56	74	93	73	77	89	85	76	96	91	78	
	Total number of detected trees [%]	16	39	91	52	66	30	53	58	69	71	81	53
	False detected trees [%]	1	1	0	0	7	9	12	19	13	8	12	7

Table 1. Detection of trees in the reference plots